

Fabrication of Nanosized Reactive Nickel Oxide Composite Particles for Degradation of Textile Dye

S. Akhtar*, M. A. Alam, H. Ahmad

Department of Chemistry, Rajshahi University, Rajshahi 6205, Bangladesh

Received 31 May 2017, accepted in final revised form 15 October 2017

Abstract

In this research we focused on to develop new nanocomposite materials that have capacity to de-colorize and degrade industrial effluent. At first NiO nanoparticle were synthesized by simple liquid phase process using $\text{Ni}(\text{NO}_3)_2 \cdot 6\text{H}_2\text{O}$ and NH_4OH followed by calcinations of the produced $\text{Ni}(\text{OH})_2$ as precursor at 400°C . NiO nanoparticles were modified to produce NiO/SiO₂ nanocomposite particles. Finally tri-layered inorganic/organic nanocomposite particles were prepared by seeded polymerization of epoxide functional monomer, glycidyl methacrylate (GMA) in presence of NiO/SiO₂ nanocomposite seed particles. The composite particles were named as NiO/SiO₂/PGMA and the obtained particles were utilized as a photocatalyst for the UV-light assisted degradation of congo red (CR), a model azo dye. Degradation efficiency decreased with the increase of initial CR concentration and a maximum efficiency of 100% was achieved when the CR concentration was 40 mg/L.

Keywords: Nanoparticle; Epoxide functionality; Seeded polymerization; Photocatalyst.

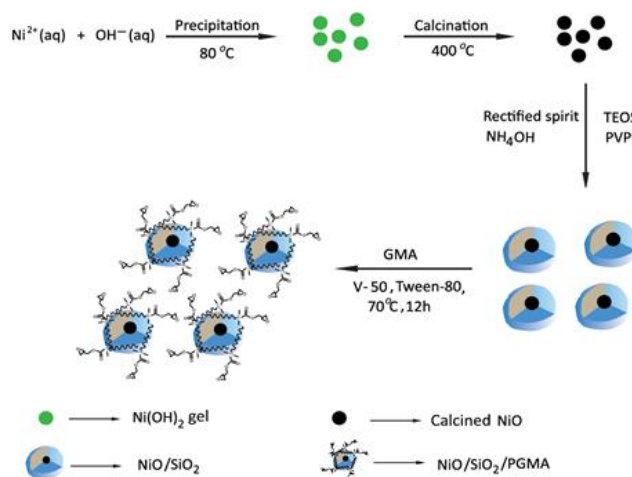
© 2017 JSR Publications. ISSN: 2070-0237 (Print); 2070-0245 (Online). All rights reserved.
doi: <http://dx.doi.org/10.3329/jsr.v9i4.32726> J. Sci. Res. 9 (4), 413-420 (2017)

1. Introduction

Today, more than 10,000 commercial dyes are available in the market. Nearly one million tons of commercial dyes are produced per year. About 10% of the produced dyes are released in environment and natural resources as dyestuff waste [1]. Various adsorbents such as alum, activated carbon, ferric chloride (FeCl_3), CaCl_2 -modified bentonite have been developed. But these adsorbents are being expensive and unable to reduce the toxicity of dyes down to below optimum level and hence the environmental problem remain unsolved [2,3]. In order to overcome this problem, semiconductors can be a good option for the photocatalytic degradation of organic dyes by utilizing visible light and oxygen available in air [4]. Among the various oxide materials, nickel oxide (NiO) is a very important semiconducting oxide material extensively used in catalysis, battery

* Corresponding author: sammi.chem.ru@gmail.com

cathodes, gas sensors, electrochromic films, and magnetic materials [5-14]. NiO is a *p*-type semiconductor characterized by a wide band gap between (3.5 eV) valence band (3.1 eV) and conduction band (- 0.5 V) that makes it suitable for photocatalysis processes [15-17]. The major drawback of the photocatalytic process is the electron/hole pair recombination. To solve this problem nanoparticles are often incorporated into a matrix materials to design nanocomposite materials. In other word nanocomposites are composites in which at least one of the phases shows dimensions in the nanometer range ($1 \text{ nm} = 10^{-9} \text{ m}$) [18]. Silica is one of the most commonly used matrix since it has great application potential in many industrial areas such as paints, catalysis, drug delivery, composite materials, and so on [19-23]. Among many other processes, Stober process was used for synthesizing NiO/SiO₂ composite particles [24]. The fabrication of hybrid inorganic/organic polymer composites offers advantages especially, when those applications depend on mechanical and surface properties as well as colloidal stability. Considering the utility of hybrid composite, epoxide functional NiO composite particles named as NiO/SiO₂/poly(glycidyl methacrylate) named NiO/SiO₂/PGMA have been fabricated according to the Scheme 1.



Scheme 1. Reaction scheme for the preparation of NiO/SiO₂/PGMA nanocomposite particles.

2. Experimental

2.1. Chemicals and instruments

GMA purchased from Fluka, Chemika, Switzerland, was passed through activated basic alumina to remove inhibitors and preserved in the refrigerator until use. Nickel nitrate hexahydrate (Ni(NO₃)₂·6H₂O) from LOBA Chem, India, and ammonium hydroxide (NH₄OH) from BDH Chemicals Ltd. Poole England were used as received. Poly(vinyl

pyrrolidone) (PVP) of molecular weight $3.6 \times 10^5 \text{ g mol}^{-1}$ from Fluka, Chemika, Switzerland, was used as a steric stabilizer. Tetraethylorthosilicate (TEOS) from Sigma Chemical Company, USA, was preserved in the refrigerator and used without purification. 2,2-Azobis (2-amidino propane) dihydrochloride (V-50) from LOBA Chem, India, was recrystallized from distilled deionized water and preserved in the refrigerator before use. Congo red (CR) from Matheson Coleman and Bell, USA was used as a model azo dye, and other chemicals used were of analytical grade.

Scanning electron microscope, SEM (LEO Electron Microscopy Ltd., UK); transmission electron microscope, TEM (Zeiss EM-912, Omega); FTIR (Perkin Elmer, FTIR-100, USA); centrifuge machine from Kokuson Corporation, Tokyo, Japan; Optima SP-300 spectrophotometer, Tokyo, Japan and microprocessor pH meter from Mettler Toledo (MP 220, Switzerland) Instruments were used in this study. Thermogravimetry (TG) analyzer (STA 8000, Perkin Elmer, Netherlands) was used to study the thermal properties.

2.2. Preparation of NiO nanoparticles

Aqueous solution (0.6 M) of $\text{Ni}(\text{NO}_3)_2 \cdot 6\text{H}_2\text{O}$ taken in a round bottomed flask dipped in an oil bath was heated at 80°C , and the temperature was gradually raised to 100°C over 2 h under magnetic stirring. 25% NH_4OH was added slowly into the solution until pH 7 was reached. The obtained green colloid was filtered with filter paper filtered and washed several times with deionized distilled water. The residual part was then dried at 100°C for 10 h to obtain the precursor, $\text{Ni}(\text{OH})_2$ powder. Finally NiO nanoparticles were obtained by calcination at 400°C for 3 h.

2.3. Preparation of NiO/SiO₂ nanocomposite particles

NiO powder (1.5 g) was dispersed in 40 g ethanol containing 0.15 g of PVP by ultrasonication for 15 min. Then ethanol (91 g), 25% ammonia solution (15 g) and TEOS (2.25 g) were added to the reaction flask containing NiO dispersion. The hydrolysis of TEOS was carried out under mechanical stirring for 8 h at 70°C in a nitrogen atmosphere. Grey colored emulsion was washed three times and finally dispersed in distilled water.

2.4. Preparation of NiO/SiO₂/PGMA nanocomposite particles

10.49 g of washed NiO/SiO₂ nanocomposite dispersion (solid 1 g), GMA (0.5 or 1.0 g), and 80 g of deionized distilled water were transferred to a three-necked round-bottomed flask dipped in a thermostat water bath maintained at 70°C . V-50 (0.02g) dissolved in distilled water was immediately added to the reaction flask, and the polymerization was carried out under a nitrogen atmosphere while the reaction was continued for 12 h. The produced composite polymer particles were centrifuged at 5000 rpm and washed three times with distilled water to remove any unreacted monomer and initiator fragments.

2.5. Point of zero charge (PZC) for NiO/SiO₂/PGMA nanocomposite particles

PZC values for NiO/SiO₂/PGMA nanocomposite particles were determined in 0.1 M NaNO₃ solution. The composite sample (0.1 g) and 0.1 M NaNO₃ (20 mL) were mixed in 100 mL beaker and the pH of the suspension was immediately adjusted to an initial pH values of 3, 6, 7, 8, 9 respectively using either diluted HNO₃ or NaOH solutions. The beaker was covered with aluminium foil and the mixture was stirred for 24 h at room temperature. The final pH of each mixture was recorded and the Δ pH values were plotted against the initial pH values. The initial pH of 7.0 at which Δ pH is zero was taken as the PZC.

2.6. Photocatalytic degradation of congo red (CR)

Photocatalytic degradation of CR was carried out at room temperature. Photocatalytic experiments were performed with a laboratory constructed “illumination box”. The obtained NiO/SiO₂/PGMA nanocomposite particles (0.05 g) were added to the aqueous dye solution and the total volume was adjusted to 50 mL with the pH value adjusted at 7.0. Before the irradiation, the reaction systems were magnetically stirred in the dark for 30 min to reach the adsorption balance. Next, the UV lamp (8 W) placed 10 cm above the sample was switched on to initiate the degradation reaction and stirring was continued during irradiation. Sample aliquots of ~10 mL were collected at a regular time interval and immediately centrifuged at 5000 rpm for 10 min to completely remove the composite particles. The centrifugation of the supernatant was repeated at the same rpm to remove any remaining dust particles. The concentration of the dye was measured by a visible spectrophotometer at the wavelength of maximum absorbance (500 nm).

3. Results and Discussion

Fig. 1 shows the FTIR spectra of NiO nanoparticles, NiO/SiO₂ and NiO/SiO₂/PGMA nanocomposite particles. The FTIR spectrum of functional NiO shows broad absorption signal in the region 250-870 cm⁻¹ which indicates the formation of metal-oxygen bond (Ni-O). In the spectrum of NiO/SiO₂ nanocomposite particles the intense signal at 1072 cm⁻¹ confirms the formation of Si—O—Si bonds. Irrespective of GMA content in the recipe both spectra of NiO/SiO₂/PGMA composite particles exhibit the same appearance. The new signal due to aliphatic —CH stretching vibration appeared in the region 2953 cm⁻¹. The small shoulder peak at 1751 cm⁻¹ corresponds to the stretching vibration of ester carbonyl group derived from GMA. The characteristic absorption signal attributes to epoxide group not visible, possibly overlapped with the strong signal from Si—O—Si bonds in the same region (950-1050 cm⁻¹). However, the overall relative results confirm the formation of epoxide functional NiO/SiO₂ nanocomposite particles.

The morphologies of NiO nanoparticles, NiO/SiO₂ and NiO/SiO₂/PGMA nanocomposite particles were confirmed by TEM image analysis (Fig. 2). Average size of

individual NiO particles is around 60 nm. NiO/SiO₂ nanocomposite particles possess hairy and porous structure. The seeded polymerization of GMA produces morphological change as the surface of NiO/SiO₂/PGMA nanocomposite particles become more compact and spherical.

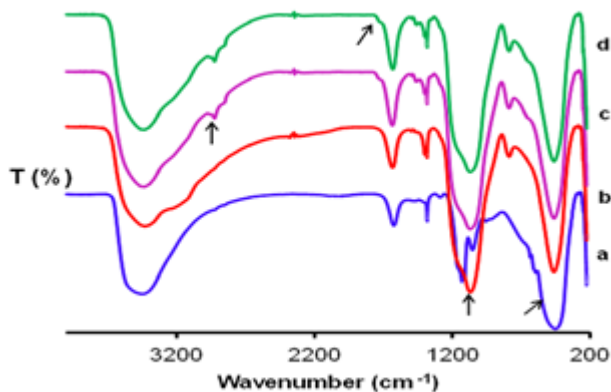


Fig. 1. FTIR spectra of a) NiO nanoparticles, b) NiO/SiO₂ and NiO/SiO₂/PGMA nanocomposite particles (c, d) prepared with different NiO/SiO₂ to PGMA ratios: c) 1/0.5 and d) 1/1.

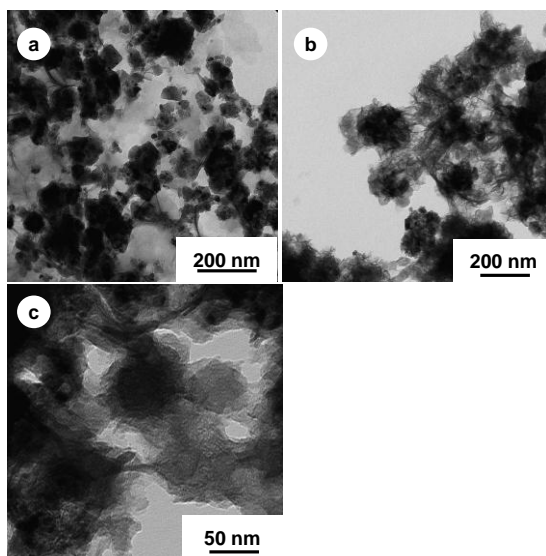


Fig. 2. TEM images of (a) NiO nanoparticles, (b) NiO/SiO₂ and (c) NiO/SiO₂/PGMA nanocomposite particles.

TGA was used to confirm the incorporation of organic polymer in hybrid composite particles. TGA curves as illustrated in Fig. 3 show that compared to bare NiO

nanoparticles a small and gradual weight loss occurs in NiO/SiO₂ nanocomposite seed particles. This weight loss represents the inclusion of organic fraction of PVP stabilizer in NiO/SiO₂ composite seed particles. It is also observed that compared to NiO/SiO₂ composite particles seeded polymerization of GMA produced a big sharp transition in NiO/SiO₂/PGMA composite particles. Which again confirms the modification of NiO with epoxide functional PGMA.

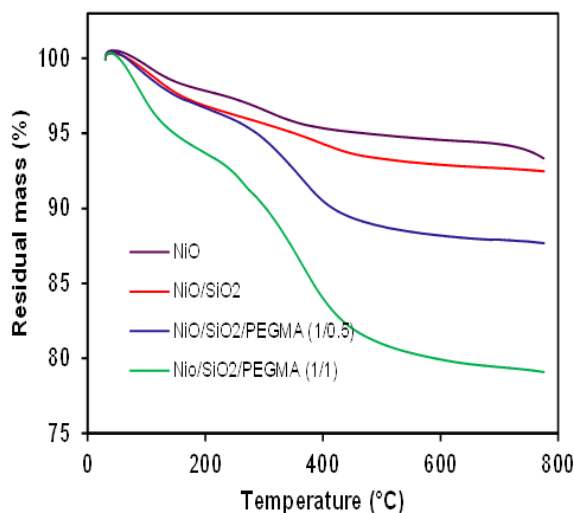


Fig. 3. TGA thermograms of NiO nanoparticles, NiO/SiO₂ and NiO/SiO₂/PGMA nanocomposite particles.

The effects of initial dye concentration and irradiation time on the degradation of CR at pH 7.0 (PZC) were studied in presence of fixed amount (0.05 g) of NiO/SiO₂/PGMA nanocomposite particles. Fig. 4A absorbance decreases sharply within 10 min of irradiation and then decreases only slowly. The slow but gradual decrease in absorbance with irradiation time indicates the disappearance of color due to the degradation of CR and thereby confirms photocatalytic activity of NiO/SiO₂/PGMA nanocomposite particles. It is also evident that the percentage of degradation decreases with the increase of initial dye concentration (Fig. 4B). The percentage of degradation of CR was calculated to be 100% at initial dye concentration of 40 mg L⁻¹. The presence of polymeric epoxide layer improved the localization of CR via hydrophobic interaction, hydrogen bonding and formation of covalent linkage with -NH₂ groups of dye molecules. When the dye solution containing the nanocomposite particles is irradiated with UV light, NiO is photoexcited by interaction and produced electrons (e_{CB}⁻) in conduction band and holes (h_{VB}⁺) in valence bands. Some of these electron hole pairs are recombined and the remaining electron hole pairs generated hydroxyl (•OH) and superoxide anion (•O₂⁻) radicals by reaction with water and molecular oxygen. Both hydroxyl (•OH) and superoxide anion (•O₂⁻) radicals

are strong oxidizing agents and therefore would oxidize the dye molecules until complete mineralization.

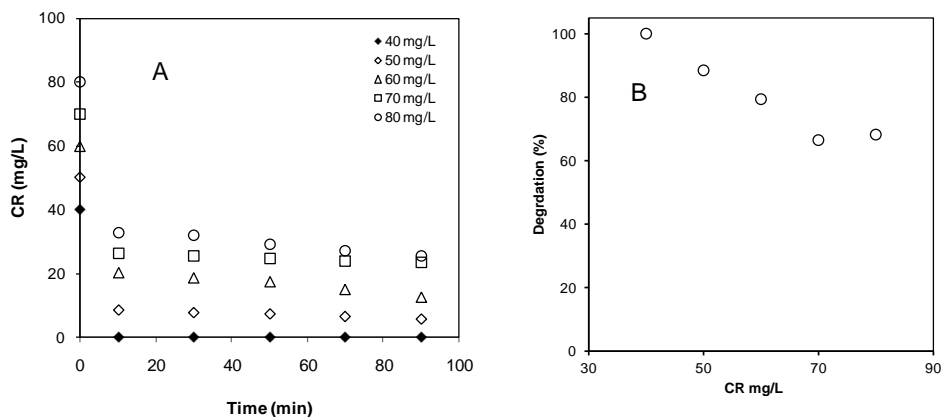


Fig. 4. A) Irradiation time dependent concentration variation for the photodegradation of CR having different initial concentrations in presence of fixed dose (0.05 g) of NiO/SiO₂/PGMA nanocomposite particles. B) Percentage of degradation at different initial concentrations of CR in presence of fixed dose (0.05 g) of NiO/SiO₂/PGMA nanocomposite particles. Conditions: pH 7; temperature, 30°C; total volume, 50 mL.

5. Conclusion

Nanosized reactive NiO nanocomposite particles named as NiO/SiO₂/PGMA were prepared by a simple three step process. NiO nanoparticles were first prepared by liquid-phase process. NiO nanoparticles were then modified with SiO₂ layer and finally seeded polymerization of GMA was carried out in presence of NiO/SiO₂ nanocomposite seed particles. The encapsulation of NiO was confirmed by electron micrographs, FTIR, XRD, EDX and TGA analyses. Photocatalytic activity of NiO/SiO₂/PGMA composite particles was confirmed by UV light driven degradation of CR dye.

References

1. J. P. Jadhav, S. S. Phugar, R. S. Dhanve, and S. B. Jadhav, *Biodegradation* **22**, 453 (2010). <https://doi.org/10.1007/s10532-009-9315-6>
2. N. Kannan and M. Meenakshisundaram, *Water, Air, Soil Pollut.* **138**, 289 (2002). <https://doi.org/10.1023/A:1015551413378>
3. P. M. K. Reddy, S. Mahammadunnisa, B. Ramaraju, B. Sreedhar, and C. Subrahmanyam, *Environ. Sci. Pollut. Res.* **20**, 4111 (2013). <https://doi.org/10.1007/s11356-012-1360-8>
4. C. Chen, W. Ma, and J. Zhao, *Chem. Soc. Rev.* **39**, 4206 (2010). <https://doi.org/10.1039/b921692h>
5. M. Yoshio, Y. Todorov, K. Yamato, H. Noguchi, J. Itoh, M. Okada, and T. Mouri, *J. Power Sources* **74**, 4 (1998). [https://doi.org/10.1016/S0378-7753\(98\)00011-1](https://doi.org/10.1016/S0378-7753(98)00011-1)
6. R. Alcantara, P. Lavela, J. L. Tirado, R. Stoyanova, and E. Zhecheva, *J. Electrochem. Soc.* **145**, 730 (1998). <https://doi.org/10.1149/1.1838338>

7. J. Park, E. Kang, S. U. Son, H. M. Park, M. K. Lee, J. Kim, K. W. Kim, H. J. Noh, J. H. Park, C. J. Bae, J.-G. Park, and T. Hyeon, *Adv. Mater.* **17**, 429 (2005).
<https://doi.org/10.1002/adma.200400611>
8. X. Wang, L. Li, Y. G. Zhang, S. T. Wang, Z. D. Zhang, L. F. Fei, and Y. T. Qian, *Cryst. Growth. Des.* **6**, 2163 (2006). <https://doi.org/10.1021/cg060156w>
9. M. C. A. Fantini, F. F. Ferreira, and A. Gorenstein, *Solid State Ionics* **512**, 867 (2002).
[https://doi.org/10.1016/S0167-2738\(02\)00387-9](https://doi.org/10.1016/S0167-2738(02)00387-9)
10. J. Bandara and H. Weerasinghe, *Sol. Energy Mater. Sol. Cells* **85**, 385 (2005).
<https://doi.org/10.1016/j.solmat.2004.05.010>
11. B. Huang, Q. C. Yu, H. M. Wang, G. Chen, and K. A. Hu, *J. Power Source* **137**, 163 (2004).
<https://doi.org/10.1016/j.jpowsour.2004.05.015>
12. I. Hotovy, V. Rehacek, P. Siciliano, S. Capone, and L. Spiess, *Thin Solid Film* **418**, 9 (2002).
[https://doi.org/10.1016/S0040-6090\(02\)00579-5](https://doi.org/10.1016/S0040-6090(02)00579-5)
13. E. L. Mille and R. E. Rocheleau, *J. Electrochem. Soc.* **144**, 3072 (1997).
<https://doi.org/10.1149/1.1837961>
14. Z. Xu, M. Li, J. Y. Zhang, L. Chang, R. Q. Zhou, and Z. T. Duan, *Appl. Catal. A: General* **213**, 65 (2001). [https://doi.org/10.1016/S0926-860X\(00\)00881-4](https://doi.org/10.1016/S0926-860X(00)00881-4)
15. Y. Ju-Nam and J. R. Lead, *Sci. Total Environ.* **400**, 396 (2008).
<https://doi.org/10.1016/j.scitotenv.2008.06.042>
16. D. H. Yang, C. S. Park, J. H. Min, M. H. Oh, Y. S. Yoon, S. W. Lee, and J. S. Shin, *Curr. Appl. Phys.* **9**, 132 (2009). <https://doi.org/10.1016/j.cap.2008.12.057>
17. F. Augusto, E. Carasek, R. G. C. Silva, S. R. Rivellino, A. D. Batista, and E. A. Martendal, *J. Chromatography A* **1217**, 2533 (2010). <https://doi.org/10.1016/j.chroma.2009.12.033>
18. R. Roy, R. A. Roy, and D. M. Roy, *Mater. Lett.* **4**, 323 (1986). [https://doi.org/10.1016/0167-577X\(86\)90063-7](https://doi.org/10.1016/0167-577X(86)90063-7)
19. Y. Lu, J. Mcllellan, and Y. Xia, *Langmuir* **20**, 3464 (2004). <https://doi.org/10.1021/la036245h>
20. K. Kamata, Y. Lu, and Y. Xia, *J. Am. Chem. Soc.* **125**, 2384 (2003).
<https://doi.org/10.1021/ja0292849>
21. G. Decher, *Science* **277**, 1232 (1997). <https://doi.org/10.1126/science.277.5330.1232>
22. I. Tissot, C. Novat, F. Lefebvre, and E. Bourgeat-Lami, *Macromolecules* **34**, 5737 (2001).
<https://doi.org/10.1021/ma010278r>
23. C. Graf, D. Vossen, and A. Imhof, *Langmuir* **19**, 6693 (2003).
<https://doi.org/10.1021/la0347859>
24. W. Stöber, A. Fink, and E. Bohn, *J. Colloid Interface Sci.* **26**, 62 (1968).
[https://doi.org/10.1016/0021-9797\(68\)90272-5](https://doi.org/10.1016/0021-9797(68)90272-5)